Electric and Electromagnetic Signals emitted from rocks under stress up to fracture. Experimental results.

I. STAVRAKAS, D. TRIANTIS, C. ANASTASIADIS
Technological Educational Institution of Athens
12210, Athens,
GREECE

A. NARDI , R. CARLUCCIO
Istituto Nazionale di Geofisica e Vulcanologia
Viale Pinturicchio, 23/e
00196 - Roma
ITALY

F. VALLIANATOS
Technological Educational Institution of Crete
Laboratory of Geophysics and Seismology
3 Romanou Str., Chania, Crete
GREECE

Abstract: - The application of mechanical stress on a rock sample can stimulate electric and electromagnetic signal emissions. Such emissions can be detected experimentally. In this work, experiments that show up Electric and Electromagnetic signal emissions during the application of mechanical stress with various modes, are described. The experimental results manifest that such Electric and Electromagnetic signals can be used as precursors of the upcoming failure.

Key-Words: - Electric signals, Electromagnetic precursors, Pressure, Stress, Rocks.

1 Introduction

The phenomena of Electric and Electromagnetic (EM) emissions that are met when a material is about to fail due to mechanical reasons are most interesting. Especially when the material under study belongs to the class of brittle geomaterials and such phenomena are promising candidates of earthquake precursors. During the development of the deformation, when a geomaterial suffers externally applied stress, various mechanisms contribute to the generation of electric signal emission. These mechanisms are related to the crack generation and propagation processes [1-4]. Although important similarities exist between the fracture of a pristine rock and an earthquake rupture, there are also important differences [5].

This concept is documented and efforts focus on two main paths. Theoretical works have been introduced in order to model the underlying physical mechanisms that can generate transient electric and EM signals [4-9]; while concurrently several experimental works have been performed to investigate in detail the characteristics of such electric and EM emissions [10-17]. The proposed theoretical models implicate various stimulus for the currents generated during stress application on geomaterials. The piezoelectric and electrokinetic effects have been studied theoretically [18,19] and experimentally [10,20-22] as potential sources of the electric and EM emissions but were not applicable for quartz free and low porosity materials without physical humidity. The dominant theory that is applicable for materials that are met in the crust of the Earth concerns electric current production from crack opening process. This process is best described by a summation of the underlying physical mechanisms called Moving Charged Dislocations (MCD) model [23-26].

Several experimental works were conducted to evaluate the proposed theoretical models. A critical factor of these experimental works is the selection of the material under test. Some of the used materials exhibit high quartz content favoring piezoelectric effect and others contain in their volume many connected pores favoring the electrokinetic effect since their viscosity permits fluid transportation. Electric emissions from materials that exhibit low quartz content and porosity can only be interpreted by the MCD model [14-17].

In the present work experimental results that connect the time-varying mechanical stress that was applied on rock samples to the emitted electric and EM signals are presented.

2 Experimental Techniques and results.

2.1 Electrical Measurements

This work describes the experimental results when marble samples were subjected to stress of various modes. The marble was selected as a typical metamorphic geo-material that can be characterised as quartz-free with extremely low porosity and physical water content, thus the influence of piezoelectric and electrokinetic effects can be neglected. The used marbles were collected from Mt. Penteli at Attica, Greece.

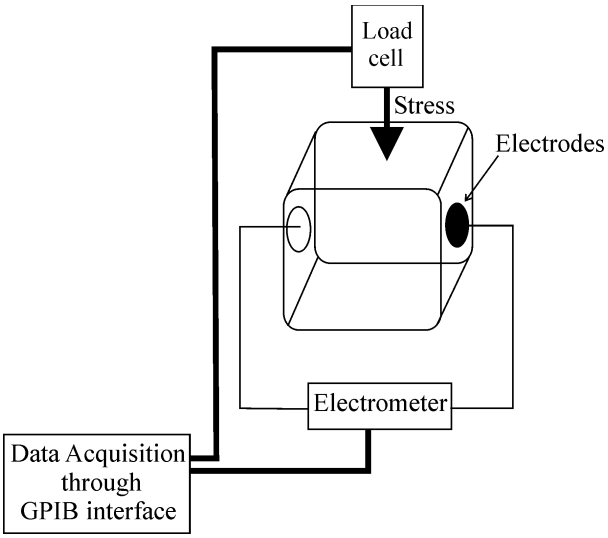

FIGURE 1: The experimental apparatus for electrical measurements

The experiments were conducted in a Faraday shield to prevent electric noise from affecting the recordings. The noise-protected system comprised a uniaxial hydraulic load machine (Enerpac–RC106) that applied compressive stress to the marble samples. Each sample was placed between two thin teflon plates, in the direction of stress, in order to provide electrical insulation. The values of the externally applied stress were measured using a load cell. A pair of electrodes was attached to the marble sample, using conductive paste. The electrodes were attached in a direction perpendicular to the axis of the applied stress (see Figure 1). For electrical measurements a sensitive programmable electrometer Keithley 617 was used. All the recordings originating from the load cell and the electrometer, were stored in a PC through a GPIB interface. The recorded weak electric current emissions are known as Pressure Stimulated Currents (PSC).

During the experiments the stress were applied with two modes. At the first mode the sample suffered stress with constant stress rate. These experiments were repeated for various stress rates. At the second mode the samples suffered stress from low levels up to fracture and the stress rate was initially high and continuously decreasing until the fracture. PSC measurements were conducted during these modes of stress application.

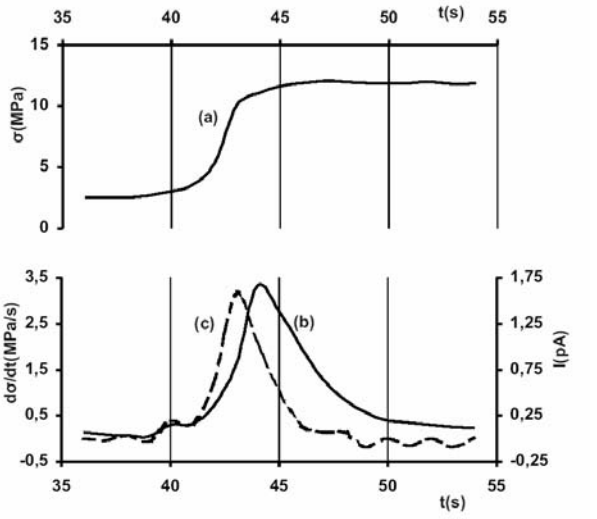

FIGURE 2. Time recordings of: single variation of stress (curve a), the emitted PSC (curve b), the corresponding stress rate (curve c).

Figure 2 is a typical recording of PSC emission (curve a) during a stress stepwise increase (curve b) in low stress levels that correspond to the linear deformation range [27]. Curve (c) shows the corresponding stress rate which, evidently, has the same form with the emitted PSC. A proportionality factor γ can be used to describe the relation

between the emitted PSC and the applied mechanical stress rate as follows:

$$\gamma = \frac{I_{\max}}{\left(d\sigma/dt\right)_{\max}} \qquad (1)$$

where I_{max} is the peak PSC value and $(d\sigma/dt)_{max}$ is the corresponding peak stress rate.

A large number of measurements of such PSC and stress rate pairs were collected for stress values that start from the early stress levels up to the vicinity of fracture. This process allows the experimental determination of γ and its variation as a function of the applied stress by using Equation (1).

Figure 3 demonstrates the dependence of γ on the normalized stress σ/σ_{max}, where σ_{max} is the sample's ultimate compressional stress strength and σ is the average stress during the stepwise increase and is practically equal to the instantaneous stress at the time when the maximum stress rate $(d\sigma/dt)_{max}$ is exerted. Figure 3 clearly demonstrates that when the applied stress is lower than $0.6\sigma_{max}$, the value of γ remains practically constant. According the the stress-strain curve of the used marble type, as long as the normalised applied stress σ/σ_{max} is lower than 0.6 the deformation is linearly related to the stress and in this range the the material behaves elastically and the Young's modulus remains constant.

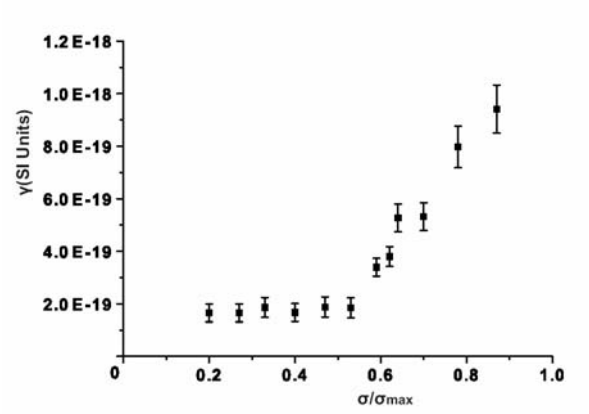

FIGURE 3: Scaling factor γ with respect to the normalized stress.

When the normalized stress exceeds 0.6 the material gradually enters the plastic deformation range where the Young modulus is continuously decreasing with respect to the increasing stress. According to the MCD model the emitted PSC can be describedby the following law:

$$I \propto \frac{1}{Y_{eff}} \cdot \frac{d\sigma}{dt} \qquad (2)$$

where Y_{eff} is the effective value of the Young's modulus. and from Equations (1) and (2) it is evident that

$$\gamma \propto \frac{1}{Y_{eff}},$$

Figure 4 represents the temporal behaviour of the PSC when a marble sample is compressed uniaxially at a constant stress rate of 20kPa/s up to the fracture while the inset diagram show the variation of the PSC with respect to the normalized stress. The PSC signal was recorded when the normalised stress exceeded a value of approximately 0.7. At this stress range irreversible structural changes occur due to plastic behaviour of the material. This observation has been verified repeatedly [14, 29-31] since at approximately such stress values correspond to the beginning of the non-linear range of the material where changes in structure are irreversible due to microcracks taking place [32-33]. In this range Y_{eff} is gradually lower than Y_0. The normalised stress curve at values exceeding 0.7 exhibit a smooth ascending (according to Equation 2), and it seems to reach a maximum value slightly before fracture. The peak is not clear because the process develops quickly as the stress increase rate is high and the time elapse corresponding to the range $0.9<\sigma/\sigma_{max}<1.0$ is relatively short.

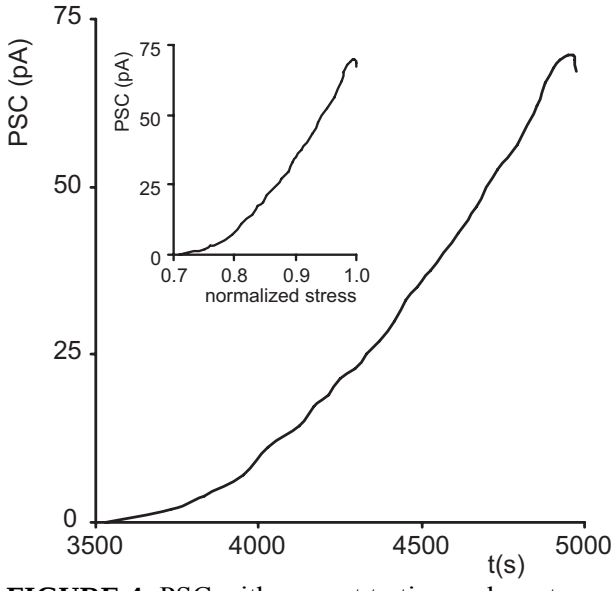

FIGURE 4: PSC with respect to time, when stress at a constant rate is applied. The inset diagram shows the PSC vs. normalized stress.

In order to show the peak in detail during the fracture process, uniaxial compression at constant deformation rate was applied. Figure 5 depicts the temporal recording of PSC when the marble sample

is subjected to an increase of the uniaxial compression at a constant deformation rate of $0.5\,\mu m/s$. In the same diagram the temporal variation of the normalized stress s is represented too. When the material enters the non-linear deformation range (σ/σ_{max}>0.7) the stress rate continuously decreases, and diminishes at σ=1, when the sample fails. As can be seen in Figure 5 the PSC peak at fracture is clearly distinguished. The emitted PSC acquires a maximum value and consequently decreases; this corresponds to a decrease of the PSC rate which becomes continuously smaller and slightly before fracture ($\sigma/\sigma_{max} \approx 0.98$) the PSC gets to a maximum and an abrupt decrease follows.

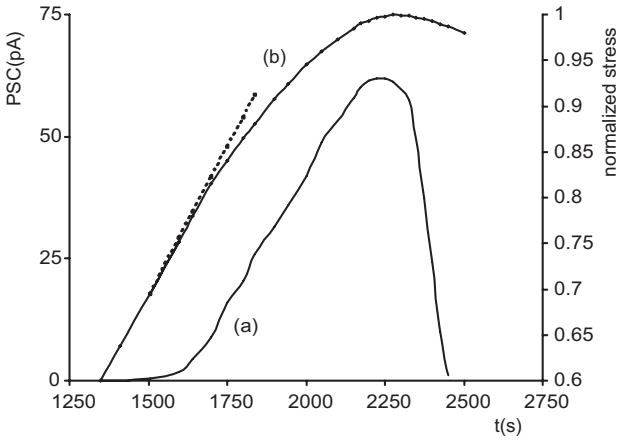

FIGURE 5: Detailed representation of the temporal variations of both PSC (curve a) and normalized stress applied on a marble sample (curve b) while the deformation rate is kept constant.

2.2 Electromagnetic Measurements

During these experiments [34-37] the electromagnetic emission by rock samples was measured from 14 different lithologies: among these limestone, lava, granite, metamorphic rock and even concrete.

The samples, all cut in parallelepiped shapes of uniform dimensions and fixed height (x,y,z: 10,10,10 and 8,8,10 cm), have been subjected to uni-axial (z) compression up to material fracture by means of a hydraulic press operated in regime of constant force over time.

To detect the electric part of the EM field an active antenna that operates on the VLF band (0.8 – 12 kHz) was used. It was positioned at a fixed distance of 20 cm from the samples centre, protected by a plastic shield from rock debris. The press movement was indirectly monitored by a capacitance meter acting on a condenser built on the press moving plate (see figure 6). This value, together with audible sound from rock and VLF signals were synchronously recorded by multi-channel digital sampler.

A typical VLF–audio measure is reported in figure 7: From a qualitative point of view, all measured signals are short pulses or pulse clusters (section a) that on a larger timescale define the observed complex time behaviour (section b).

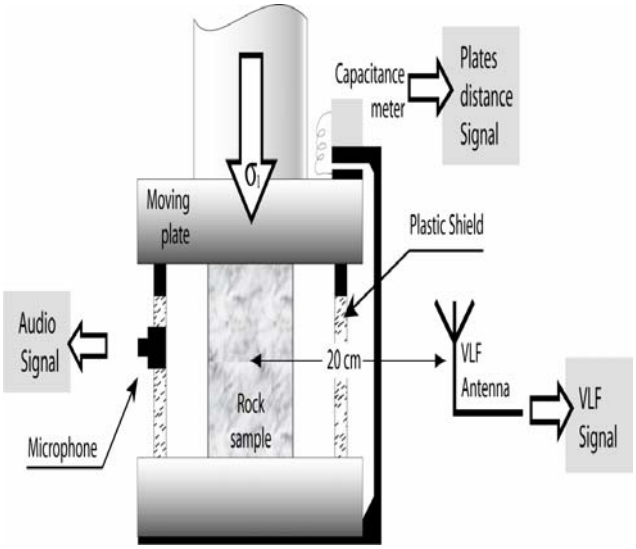

FIGURE 6: The experimental apparatus for VLF electromagnetic measurements.

The VLF signals observed can be qualitatively categorized in two main classes: Orderly and Disorderly Impulsive sequences. (OIS and DIS). If we normalize the events time measures with the time-to-rupture in a timeline ranging from 0 to 100%, the OIS usually appear in the first half (0-50) of the timeline and seem to consist of ordered packets of high frequency pulses arranged in time-repeating patterns. Figure 8 shows a typical OIS sequence. The upper half shows the detailed structure of the packets that appear almost regularly for the entire sequence (lower part).

The DIS are usually seen in the second part of the timeline (from roughly 40-50% on) and seem to be random distributed over time with the tendency of creating crowded clusters of increasing density while approaching to failure. These are the typical peaks seen in the above time graphs of figure 7a. In part b of the same figure is seen how the DIS peaks amount grows up to the reaching of the so called "paroxysmal" sequence that precludes to sample rupture. Figure 9, finally, shows where usually DIS

and OIS signal are located in the measured timeline, in both amplitude and frequency domain.

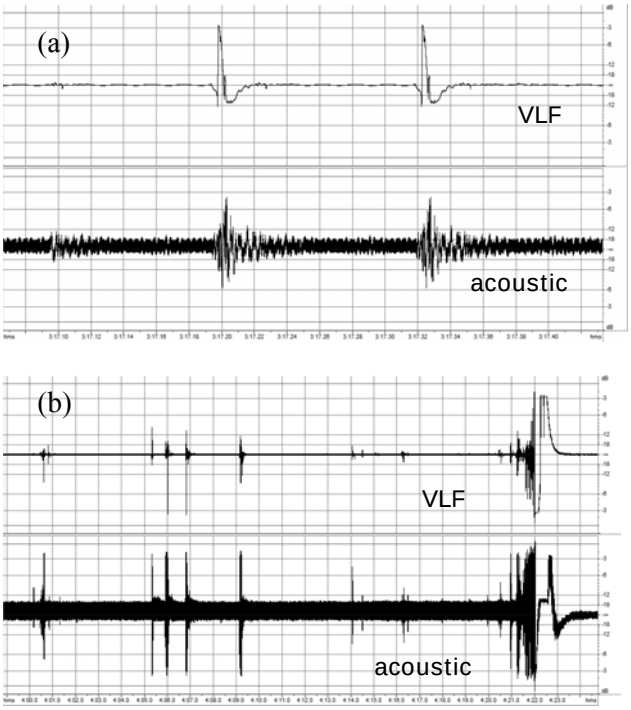

FIGURE 7: Typical DIS pattern of signals observed during the stress of the rock.

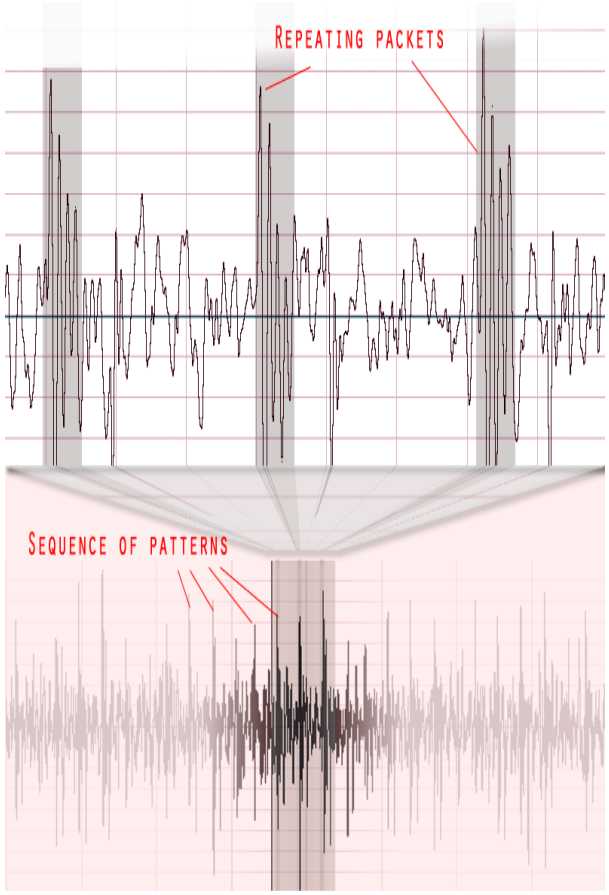

FIGURE 8: A typical OIS sequence

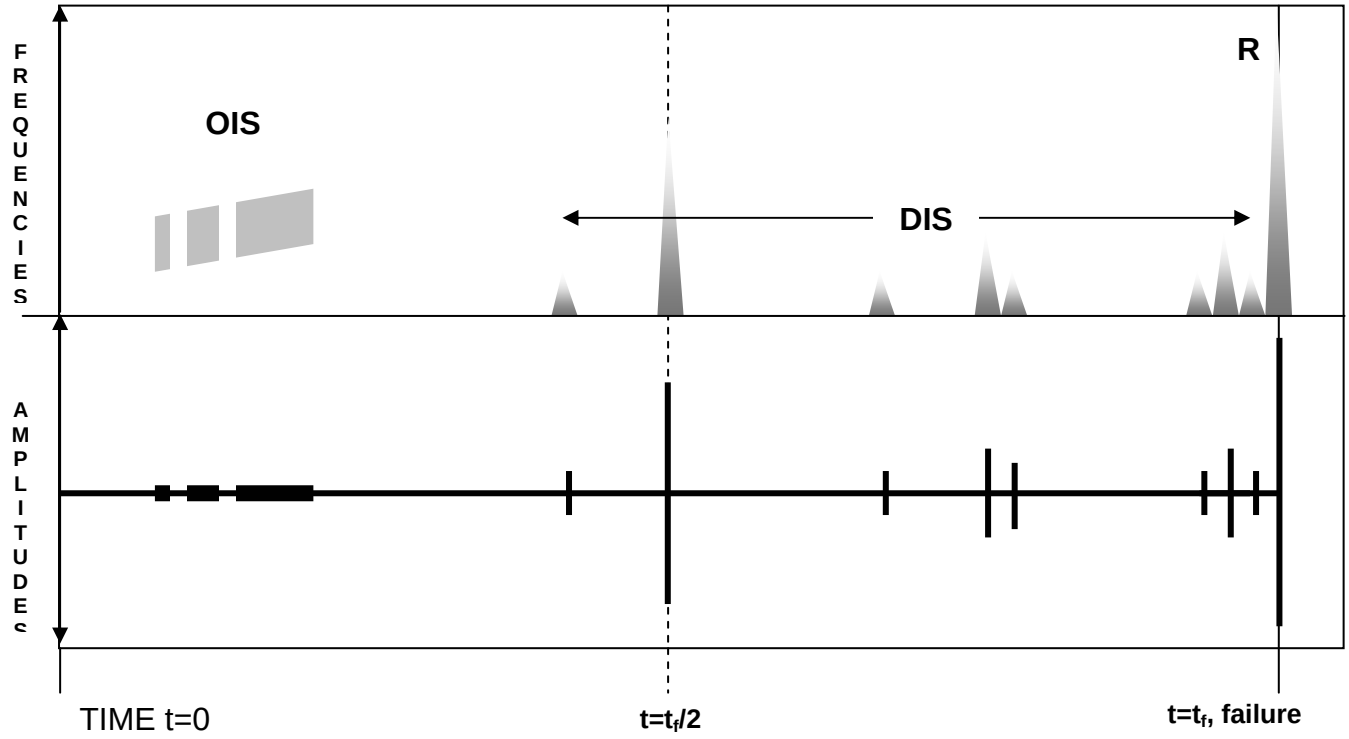

FIGURE 9: Time chart of DIS and OIS signal appears in both amplitude and frequency domains

3. Concluding Remarks.

In the above described experiments it was observed that rock samples respond to compressional stress emitting electric and VLF electromagnetic signals. The electric signals support the ideas of MCD model while the VLF electromagnetic ones present a structure that enables the classification in two categories, the so called OIDs and DIS.

References:

[1] M. Hayakawa, (Editor) *Electromagnetic phenomena related to earthquake prediction*, Terra Scientific Publishing, 1999.

[2] M. Hayakawa and Y. Fujinawa, (Editors), *Electromagnetic Phenomena Related to Earthquake Prediction*, Terra Scientific Publishing, Company, Tokyo, 1994.

[3] M. Hayakawa and O.A. Molchanov (Editors), *Seismo Electromagnetics: Lithosphere-Atmosphere-Ionosphere Coupling*, TERRAPUB, Tokyo, 2002.

[4] D.A. Fiffolt, V.F. Petrenko,. and E.M.. Schulson, Preliminary study of electromagnetic emissions from cracks in ice, *Philosophical Magazine B*, 67, 1993, pp. 289.

[5] S.G. O'Keefe and D.V. Thiel, A mechanism for the production of electromagnetic radiation during fracture of Brittle materials, *Phys. Earth Plane. Inter.*, 89, 1995, pp. 127-135.

[6] V. Frid, A. Rabinovitch and D. Bahat, Fracture induced electromagnetic radiation, *Journal of physics D: applied physics*, 36, 2003, 1620-1628.

[7] G.O. Cress, B.T., Brady, and G.A. Rowell, Sources of electromagnetic radiation from fracture of rock samples in laboratory, *Geophys. Res. Lett.*, 14, 1987, pp. 331.

[8] J.W. Warwick, C. Stoker and T.R. Meyer, Radio emission associated with rock fracture : Possible application to the great Chilean earthquake of May 22, 1960, *J. Geophys. Res.*, 87, 1982, pp. 2851.

[9] T. Ogawa, K. Oike, and T. Miura, Electromagnetic radiation from rocks, *J. Geophys. Res.*, 90, 1985, pp. 6245.

[10] S. Yoshida, M. Uyeshima, and M. Nakatani, Electric potential changes associated with a slip failure of granite : Preseismic and coseismic signals, *J. Geophys. Res.*, 102, 1997, 14883.

[11] V. Hadjicontis and C. Mavromatou, Transient electric signals prior to rock failure under uniaxial compression, *Geophys. Res. Lett.*, 21, 1994, pp. 1687.

[12] V. Hadjicontis and C. Mavromatou, Laboratory investigation of electric signals preceding earthquakes, in Sir J. Lighthill (ed.), A critical review of VAN, *World Scientific*, Singapore, 1996, pp. 105-117.

[13] C. Mavromatou and V. Hadjicontis, Laboratory investigation of transient electric signals detected by VAN network in Greece, Electromagnetic Phenomena Related to Earthquake Prediction, Edited by M.Havakawa and Y.Fujinawa, *Terra Scientific Publishing Company*, Tokyo, 1994, pp 293-305.

[14] I. Stavrakas, D. Triantis, Z. Agioutantis, S. Maurigiannakis, V. Saltas, F. Vallianatos, and M. Clarke, Pressure stimulated currents in rocks and their correlation with mechanical properties, *Natural Hazards and Earth System Sciences*, 4, 2004, pp. 563–567.

[15] I. Stavrakas, C. Anastasiadis, D. Triantis and F. Vallianatos, Piezo Stimulated currents in marble samples: Precursory and concurrent – with – failure signals, *Natural Hazards and Earth System Sciences*, 3, 2003, pp. 243-247.

[16] C. Anastasiadis, D. Triantis, I. Stavrakas, F. Vallianatos, Pressure stimulated currents (PSC) in marble samples after the application of various stress modes before fracture, *Annals of Geophysics*, vol 47, No 1, 2004, pp. 21-28.

[17] F. Vallianatos, D. Triantis, A. Tzanis, C. Anastasiadis, I. Stavrakas, Electric Earthquake Precursors: From Laboratory Results to Field Observations, *Phys. Chem. Earth*, 29, 2004, pp. 339-351.

[18] D. Finkelstein, R.D. Hill and J.R. Powell, The piezoelectric theory of earthquake lightning, *J. Geophys. Res.*, 78, 1973, pp. 992-993.

[19] D.A. Lockner, M.J.S. Johnson., and J.D. Byerlee, A mechanism to explain the generation of earthquake lights, *Nature*, 302, 1983, pp. 28-33.

[20] U. Nitsan, Electromagnetic emission accompanying fracture of quartz-bearing rocks, *Geophys. Res. Lett.*, 4, 1977, pp. 333-337.

[21] S. Yoshida, M. Uyeshima and M. Nakatani, Electric potential changes associated with a slip failure of granite : Preseismic and coseismic signals, *J. Geophys. Res.*, 102, 1997, pp. 14883-14897.

[22] H. Mizutani, T. Ishido, T. Yokokura and S. Ohnishi, Electrokinetic phenomena associated with earthquakes, *Geophys. Res. Lett.*, 3, 1976, pp. 365-368.

[23] L. Jouniaux and J.P. Pozzi, Permeability dependencs of streaming potential in rocks for

various fluid conductivities, *Geophys. Res. Lett*., 22, 1995, pp.485-488.

[24] R.W. Whitworth, Charged dislocations in ionic crystals, *Advances in Physics*, 24, 1975, pp. 203-304.

[25] L. Slifkin, Seismic electric signals from displacement of charged dislocations. *Tectonophysics*, 224, 1993, pp. 149-152.

[26] F. Vallianatos and A. Tzanis, A model for the generation of precursory electric and magnetic fields associated with the deformation rate of the earthquake focus, in M. Hayakawa (ed.), *Atmospheric and Ionospheric electromagnetic phenomena associated with Earthquakes*, Terra Scientific Publishing Co, 287-305, 1999a.

[27] F. Vallianatos, and A. Tzanis, On possible scaling laws between Electric Earthquake Precursors (EEP) and Earthquake Magnitude, *Geophys. Res. Lett.*, 26, 13, 1999b, pp. 2013-2016.

[28] Z. Agioutantis, *Elements of Geomechanics - Rock Mechanics*, Ion Publishing, in Greek., 2002

[29] C. Anastasiadis, I. Stavrakas, D. Triantis and F. Vallianatos, Correlation of Pressure Stimulated Currents in rocks with the damage parameter, *Annals of Geophysics*, Vol. 50, 2007, pp. 1-6.

[30] I. Stavrakas, D. Triantis, C. Anastasiadis, Pressure Stimulated Current – PSC – emitted from marble samples when subjected to stress of various rates up to fracture, *4th WSEAS Conference on Applications of Electrical Engineering, AEE 05*, Prague, Czech Republic, 13-15 March 2005

[31] D. Triantis, I. Stavrakas, C. Anastasiadis: Comments and Remarks on the recordings of Pressure Stimulated Currents (PSC), in marble samples in the range of microcracking.", *4th WSEAS Conference on Applications of Electrical Engineering, AEE 05*, Prague, Czech Republic, 13-15 March 2005

[32] D. L. Turcotte, Newman W.I. and Shcherbakov R., Micro and macroscopic models of rock fracture. *Geophys. J. Int.*, vol. 152, 2003, pp. 718-728.

[33] J.C. Jaeger and N.G.W. Cook, Fundamentals of Rock Mechanics, London: Chapman and Hall, 593, 1979.

[34] Nardi A., Caputo M.; 2006, *A perspective electric earthquake precursor observed in the Apennines*, Bollettino di Geofisica Teorica ed Applicata, Vol. 47, n. 1-2, pp. 3-12; March – June 2006.

[35] Nardi A., Caputo M. and Chiarabba C.; 2007, *Possible electromagnetic earthquake precursors in two years of ELF-VLF monitoring in the atmosphere*, Vol. 48, n. 2, pp. 205-212; June 2007.

[36] Nardi A. (2001), *Emissioni elettromagnetiche in rocce sottoposte a sollecitazione meccanica. Un possibile precursore sismico?* – Master Thesis, University of Rome "La Sapienza".

[37] Nardi A. (2005): *Emissioni elettro-magnetiche naturali come precursori di fenomeni sismici,* PHD thesis, University of Rome "La Sapienza"